

# Hadean age for a post-magma-ocean zircon confirmed by atom-probe tomography

John W. Valley<sup>1\*</sup>, Aaron J. Cavosie<sup>1,2</sup>, Takayuki Ushikubo<sup>1</sup>, David A. Reinhard<sup>3</sup>, Daniel F. Lawrence<sup>3</sup>, David J. Larson<sup>3</sup>, Peter H. Clifton<sup>3</sup>, Thomas F. Kelly<sup>3</sup>, Simon A. Wilde<sup>4</sup>, Desmond E. Moser<sup>5</sup> and Michael J. Spicuzza<sup>1</sup>

**The only physical evidence from the earliest phases of Earth's evolution comes from zircons, ancient mineral grains that can be dated using the U–Th–Pb geochronometer<sup>1</sup>. Oxygen isotope ratios from such zircons have been used to infer when the hydrosphere and conditions habitable to life were established<sup>2,3</sup>. Chemical homogenization of Earth's crust and the existence of a magma ocean have not been dated directly, but must have occurred earlier<sup>4</sup>. However, the accuracy of the U–Pb zircon ages can plausibly be biased by poorly understood processes of intracrystalline Pb mobility<sup>5–7</sup>. Here we use atom-probe tomography<sup>8</sup> to identify and map individual atoms in the oldest concordant grain from Earth, a 4.4-Gyr-old Hadean zircon with a high-temperature overgrowth that formed about 1 Gyr after the mineral's core. Isolated nanoclusters, measuring about 10 nm and spaced 10–50 nm apart, are enriched in incompatible elements including radiogenic Pb with unusually high <sup>207</sup>Pb/<sup>206</sup>Pb ratios. We demonstrate that the length scales of these clusters make U–Pb age biasing impossible, and that they formed during the later reheating event. Our tomography data thereby confirm that any mixing event of the silicate Earth must have occurred before 4.4 Gyr ago, consistent with magma ocean formation by an early moon-forming impact<sup>4</sup> about 4.5 Gyr ago.**

Zircons older than 4.3 Gyr old are extremely rare. So far, there are published secondary-ion mass spectrometry (SIMS) data from only four terrestrial zircons, all from the Yilgarn Craton of Western Australia, indicating single-spot <sup>207</sup>Pb/<sup>206</sup>Pb ages >4.35 Gyr old<sup>9–13</sup>. These tiny detrital grains are the oldest known terrestrial samples, providing a basis for theories of crustal growth, tectonics, surface conditions and possible habitats for life on early Earth<sup>2,3,12,13</sup>. However, uncertainty about the cumulative effect of un-annealed radiation damage and mobility of radiogenic isotopes has led to questions about the reliability of ages and other geochemical characteristics of these zircons<sup>7,10,14–16</sup>.

Radiation damage can promote mobility and loss (or concentration) of radiogenic Pb in zircon<sup>17</sup>. The decay of parent atoms of <sup>238</sup>U, <sup>235</sup>U and <sup>232</sup>Th produces chains of 8, 7 and 6  $\alpha$ -decay events, respectively. Emission of  $\alpha$ -particles causes low concentrations of atomic displacements along 10–20  $\mu$ m tracks. Much more crystal-structure damage is caused by  $\alpha$ -recoil of the newly formed daughter atom, which travels 20–40 nm depending on energy<sup>5,18–20</sup>. Lead isotope mobility due to radiation damage has not previously been studied at the atomic scale and the relation of radiation damage to Pb migration is poorly understood.

Sample 01JH36-69 is a detrital zircon from weakly metamorphosed sandstone from the Jack Hills, Western Australia<sup>13,21</sup>. This zircon was imaged by scanning electron microscopy (SEM; Fig. 1) and electron backscatter diffraction (EBSD), and analysed by SIMS in 10–20- $\mu$ m-diameter spots to determine its age, oxygen three-isotope ratios and trace element compositions. Needle-like specimens were milled by focused ion beam (FIB) to dimensions of  $\sim 100 \times 100 \times 1,000$  nm for atom-probe tomography (APT) analysis;  $6 \times 10^8$  ions were field-evaporated, identified by time-of-flight mass spectrometry, and located at subnanometre scale by a position-sensitive detector with an efficiency of  $\sim 37\%$ <sup>22</sup> (Supplementary Appendix 1).

All three U–Pb SIMS analyses in the zircon core (Fig. 1) are concordant, with <sup>207</sup>Pb/<sup>206</sup>Pb ages from  $4,382 \pm 10$  to  $4,365 \pm 10$  and averaging  $4,374 \pm 6$  Myr old ( $\sim 4.4$  Gyr old; Fig. 2 and Supplementary Appendix 2A,B). The outermost 10–20  $\mu$ m rim is dated at  $\sim 3.4$  Gyr old, indicating new zircon growth at high temperatures; abundant orthogneisses of this age surround the Jack Hills<sup>23</sup>.

The two specimens analysed by APT were from the core of 01JH36-69 closest to the SIMS analysis pit that yielded the oldest age (4,382 Myr old, Fig. 1c and Supplementary Appendix 2), an undamaged region of uniform band contrast and orientation revealed by EBSD (Supplementary Appendix 6). A total of  $2 \times 10^8$  ions were detected from specimen 1 and  $4 \times 10^8$  from specimen 2. Twenty-one elements were analysed (Supplementary Appendix 3), including Zr, Si, O, Pb, Hf, U, Y, and mid- to heavy-rare earth elements (REEs).

The concentrations of Pb, Y and REEs are highly heterogeneous in both specimens (Figs 3 and 4 and Supplementary Appendices 3 and 4). Incompatible elements are concentrated in clustered domains that contain an average of 4.4 at.% Y (10.6 wt.%); Zr concentration is lower to compensate. In detail, the clusters are radially zoned with the highest concentrations of incompatible elements in the centre of each cluster (Fig. 4). The boundaries of clusters are here defined by the 3 at.% Y contour and compositions of matrix zircon outside the clusters are determined for the domain with Y < 1 at.%.

A total of 409 clusters with over 3 at.% Y are dispersed throughout the two analysed specimens, including 90 partial clusters that intersect edges of the ion-milled specimens. On the basis of a thorough evaluation of the effect of reconstruction variables, the clusters are found to be sub-equant to flattened to slightly elongate (Fig. 3, rotating three-dimensional images are in Supplementary

<sup>1</sup>WiscSIMS, NASA Astrobiology Institute, Department of Geoscience, University of Wisconsin, Madison, Wisconsin 53706, USA, <sup>2</sup>University of Puerto Rico, Mayaguez, Puerto Rico 00681, USA, <sup>3</sup>CAMECA, Madison, Wisconsin 53711, USA, <sup>4</sup>Curtin University, GPO Box U1987, Perth 6845, Western Australia, Australia, <sup>5</sup>University of Western Ontario, London, Ontario N6A 5B7, Canada. \*e-mail: valley@geology.wisc.edu

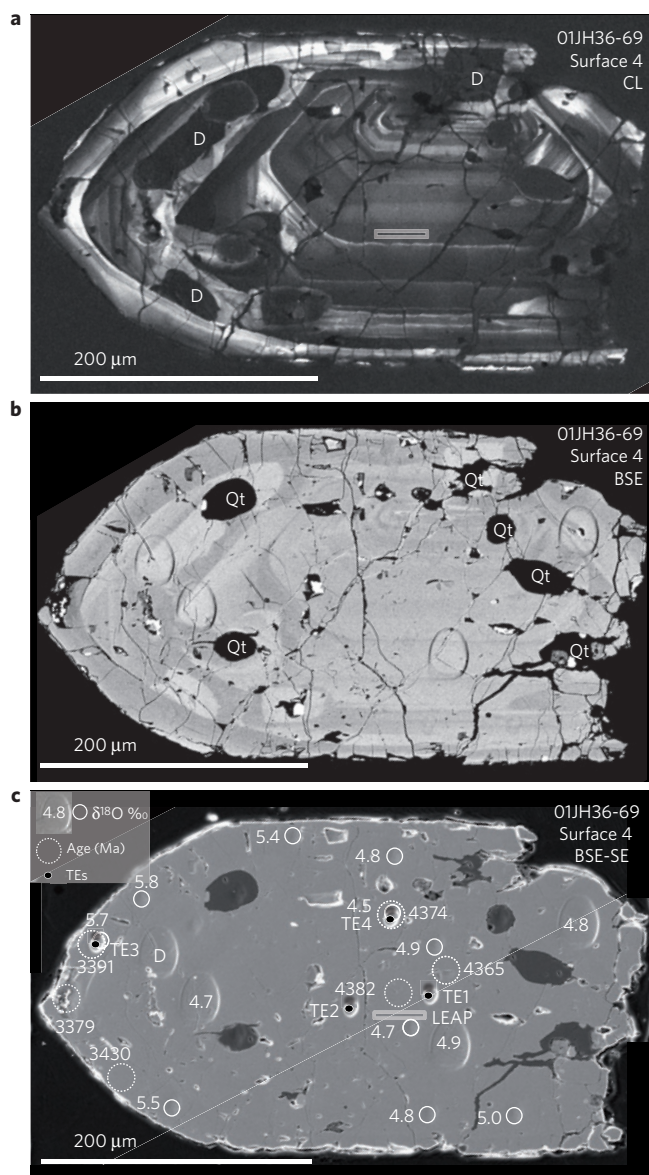


**Figure 1 | SEM images of growth zoning, inclusions and analysis spots for the 4.4-Gyr-old zircon. a–c.** Images of surface 4 of zircon 01JH36-69 are by: cathodoluminescence (CL, **a**); backscattered electrons (BSE, **b**); and combined BSE and secondary electrons (BSE-SE, **c**). Bands that are darker in cathodoluminescence and brighter in BSE are enriched in U, Pb, Y and REEs. The locations of APT specimens are shown by dots within the rectangles in **a** and **c**. SIMS pits are shown in **c**, labelled by age (Myr),  $\delta^{18}\text{O}$  (‰), or trace element analysis number (TE). Large  $\delta^{18}\text{O}$  pits in **c** were also analysed for  $\Delta^{17}\text{O}$ . D, disturbed zircon domains; Qt, quartz inclusions.

Appendix 4). The measured volumes inside the contour for  $Y = 3$  at.% for most clusters range from 125 to 500 nm<sup>3</sup>, equivalent to a 6–10-nm-diameter sphere. The abundance of  $\sim 1$  cluster per 10<sup>5</sup> nm<sup>3</sup> suggests an average spacing of  $\sim 50$  nm, which is larger than the average measured inter-cluster distance of 22 nm, indicating that the distribution is not random. The clusters seem to be in spatially related groups consistent with  $\alpha$ -recoil cascades (Supplementary Appendix 4).

The images for Pb in Fig. 3 include  $^{207}\text{Pb}^{++}$  and  $^{206}\text{Pb}^{++}$  for which no isobaric interferences are observed other than background (Supplementary Appendix 5). No peaks are detected for  $\text{Pb}^+$  and the peak for  $^{208}\text{Pb}^{++}$  is not resolved from  $^{28}\text{Si}^{16}\text{O}^+$ . Thus,

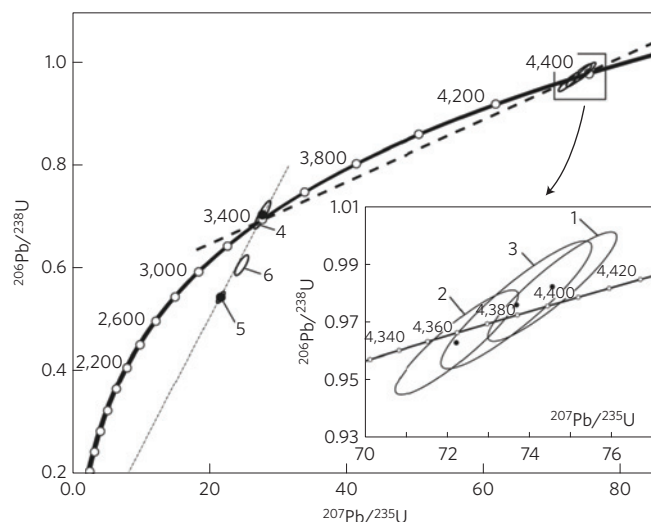


**Figure 2 | APT and SIMS U-Pb data for the 4.4-Gyr-old zircon.** U-Pb concordia diagram showing all six SIMS analyses from surface 3 of zircon 01JH36-69. Analysis locations are shown in Fig. 1c. All three analyses from the core are concordant and average 4,374 Ma. Three analyses on the thin rim fall on a discordia line (light dashes) indicating reheating and zircon growth at about 3,400 Ma. The APT  $^{207}\text{Pb}/^{206}\text{Pb}$  ratio of 1.2 defines the slope of the heavy dashed line originating from the crystallization age of 4,374 Ma. The lower intercept of this line with the curved concordia line (solid) is in agreement with the 3,400 Ma age of the overgrowth and links the formation of Pb clusters to the reheating event.

accurate concentrations can be measured only for  $^{207}\text{Pb}$  and  $^{206}\text{Pb}$ ; the additional geochronometer based on  $^{232}\text{Th}$  decay to  $^{208}\text{Pb}$  will not be considered here. No  $^{204}\text{Pb}$  (non-radiogenic) was detected in this sample, in agreement with SIMS data that show  $^{204}\text{Pb}/^{206}\text{Pb} < 0.0001$ . When only  $^{207}\text{Pb}$  and  $^{206}\text{Pb}$  are considered for the domains inside the 3-at.%-Y contours, [Pb] averages 800 ppmw (Supplementary Appendix 3; 4,400 ppmw, by weight).

The  $^{207}\text{Pb}/^{206}\text{Pb}$  ratio can be determined for different nano-domains in this zircon. If data are selected only from the volume inside the 3-at.%-Y contours of the Pb-enriched clusters, there are  $2,345 \pm 100$  atoms of  $^{206}\text{Pb}$  and  $2,942 \pm 110$  atoms of  $^{207}\text{Pb}$  detected ( $^{207}\text{Pb}/^{206}\text{Pb} = 1.2 \pm 0.05$ , 2 s.d., standard deviations) (Supplementary Appendix 2C). This contrasts with  $7,439 \pm 170$  atoms of  $^{206}\text{Pb}$  and  $2,223 \pm 100$  atoms of  $^{207}\text{Pb}$  ( $^{207}\text{Pb}/^{206}\text{Pb} = 0.30 \pm 0.05$ ) for the Pb-poor domain outside the clusters ( $Y < 1$  at.%). The total counts for the full volume collected from both specimens yield  $^{207}\text{Pb}/^{206}\text{Pb} = 0.52 \pm 0.04$ . Thus, APT detected not only heterogeneous distribution of Pb and other trace elements but also heterogeneity in the Pb isotope ratio at the nanometre scale.

Comparison of  $^{207}\text{Pb}/^{206}\text{Pb}$  ratios measured at the nanometre scale by APT in the core of zircon 01JH36-69 to those measured by SIMS at the micrometre scale provide confirmation of the age and unique information relating to the thermal history of this grain. The average bulk value of  $^{207}\text{Pb}/^{206}\text{Pb}$  by APT is in good agreement with the more precise values by SIMS ( $0.52 \pm 0.04$  versus  $0.548 \pm 0.002$ ), indicating that the Pb is radiogenic and that APT data are accurate. Precision is better by SIMS, which averages a volume of  $\sim 1,000 \mu\text{m}^3$  in zircon,  $\sim 10^5$  larger than the combined volume by APT ( $0.02 \mu\text{m}^3$ ).

Within clusters, the  $^{207}\text{Pb}/^{206}\text{Pb}$  ratios can be measured only by APT, and are unusually high, averaging 1.2. If interpreted as a conventional Pb/Pb model age (that is, projected from the origin of Fig. 2) the  $\sim 5.5$ -Gyr-old result is significantly older than the age of the Earth and clearly not correct. Uranium and Th are not

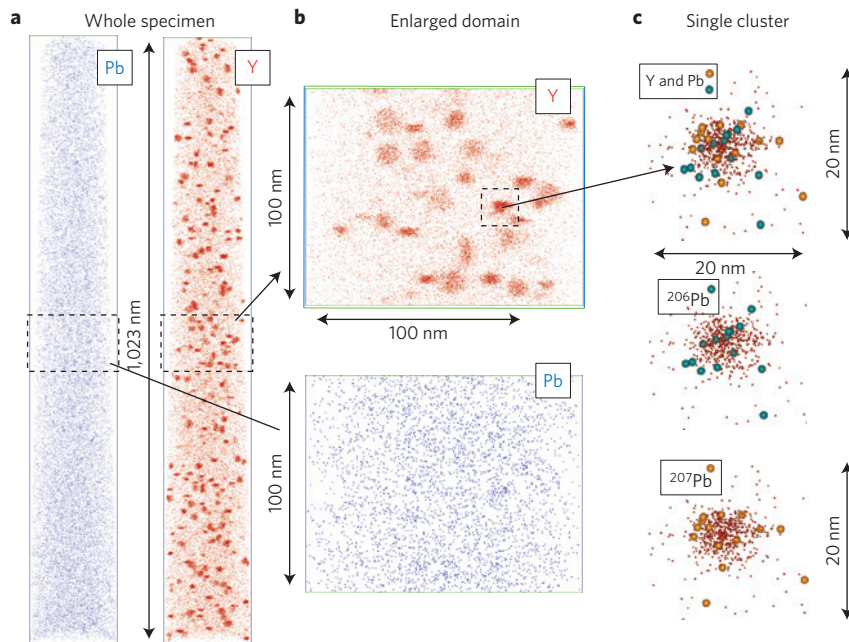


**Figure 3 | APT images of Y and Pb clusters in the 4.4-Gyr-old zircon.** The clusters of co-localized Y and Pb are from specimen 2 of zircon 01JH36-69. **a**, Projections of Y and Pb from the same 1,000-nm-long segment. The tip of the specimen points upwards. Rotating three-dimensional images are in Supplementary Appendix 4. **b**, Enlarged view of 100 nm segment of specimen 2. **c**, Individual Y and Pb atoms for one cluster: small red dots, Y; green dots,  $^{206}\text{Pb}$ ; and yellow dots,  $^{207}\text{Pb}$ . The volume shown in **c** measures 20 × 20 nm in the plane of the image by 10 nm deep.

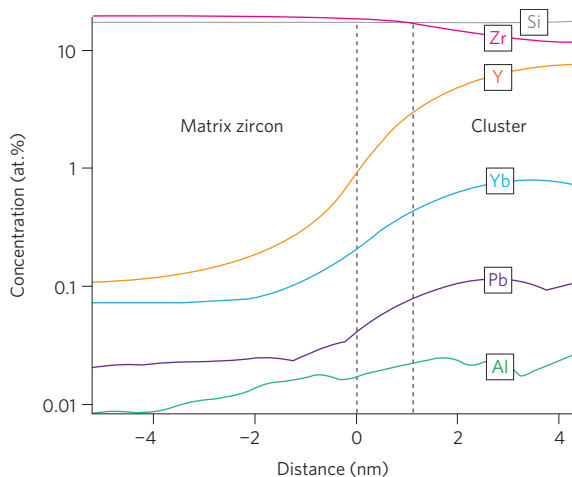


**Figure 4 | Distribution of elements in clusters in a 4.4-Gyr-old zircon.**

Proximity histogram profile of Pb, Y, Si, Zr, Yb and Al, averaged for clusters in zircon 01JH36-69 APT specimen 2. For purposes of analysis,  $^{207}\text{Pb}/^{206}\text{Pb}$  ratios are measured in the central portion of clusters where Y > 3 at.% and the matrix zircon is measured for the outer domains where Y < 1 at.%. The shell between 1 and 3% yields a mixed ratio.

concentrated in clusters, showing that most Pb inside the clusters is unsupported by parent isotopes and reinforcing the conclusion that the model age for the high  $^{207}\text{Pb}/^{206}\text{Pb}$  inside clusters has no meaning. The  $^{207}\text{Pb}/^{206}\text{Pb}$  anomaly is best explained by migration and concentration of radiogenic Pb into the clusters at a significantly later date than the formation of the zircon. If Pb mobility were assumed to have occurred during Tertiary weathering, which is known to have altered many Archean zircons from Western Australia<sup>23</sup>, that would suggest an impossibly old model age. In contrast, Pb mobility during reheating at 3.4 Gyr ago (Ga) would have concentrated radiogenic Pb formed before 3.4 Ga with higher

$^{207}\text{Pb}/^{206}\text{Pb}$  due to the greater proportion of shorter-half-life  $^{235}\text{U}$  on the early Earth.

Pb might be mobilized in zircon in two ways. If radiation damage to the crystal structure accumulated to the extent that poorly crystalline pathways exist through a zircon grain<sup>5</sup>, then even at low temperatures,  $\text{Pb}^{++}$ , which is too large for ionic substitution in zircon, can migrate quickly, especially in the presence of aqueous fluids, resulting in Pb loss (or gain). This is probably the process causing the reversely age-discordant zircon data reported previously<sup>7</sup>. However, the nanometre scale of isolated Pb clusters and the three concordant SIMS dates for the core of 01JH36-69 in this study (Fig. 2) show that there was no Pb loss at the micrometre scale of SIMS analysis, arguing against Pb mobility through a network of radiation damage. Furthermore, EBSD shows a high degree of crystallinity and little radiation damage (Supplementary Appendix 6). An alternative mechanism of Pb mobility is by volume diffusion through undamaged crystalline zircon. Diffusion to grain boundaries and into nanometre-scale domains of  $\alpha$ -recoil damage would be driven by misfit of incompatible elements (Pb, Y and REEs) in the zircon crystal structure. Diffusion is slow in undamaged zircon and diffusion distances are small, but increase with temperature and time<sup>24</sup>. A diffusion distance of 20 nm is calculated for Yb at a temperature of 800 °C in 2 million years, which is sufficient to concentrate REE in clusters during the 3.4 Ga reheating event when the zircon rim formed. Pb diffuses faster than REE, the comparable diffusion distance is 100 nm and all Pb formed from 4,374 to 3,400 Ma could move to un-annealed damaged domains. After cooling, diffusion essentially stops and younger radiogenic Pb would remain trapped in crystal defects throughout the zircon.

The  $^{207}\text{Pb}/^{206}\text{Pb}$  ratios in zircon 01JH36-69 record the age of reheating in two independent ways. SIMS analyses of the rim yield  $^{207}\text{Pb}/^{206}\text{Pb} = 0.291$  and nearly concordant U–Pb ages for crystallization of the overgrowth at 3.4 Ga. The APT measurements for domains in the zircon core that are outside clusters analyse Pb created after earlier-formed Pb was concentrated by reheating. These APT measurements yield  $^{207}\text{Pb}/^{206}\text{Pb} = 0.30$  and a model

age of 3.4 Ga, showing that effectively all radiogenic Pb formed before 3.4 Ga migrated by diffusion into clusters during the 3.4 Ga reheating event. These results are not consistent with significant reheating and Pb mobility during younger events in the Jack Hills as has been proposed by others. Subsequent radioactive decay had little effect on  $^{207}\text{Pb}/^{206}\text{Pb}$  inside the clusters because of the extreme Pb/(U+Th) ratio. We note the generality of this approach, which can be used to estimate the timing, intensity and duration of otherwise cryptic igneous and metamorphic events in zircons from other Precambrian terranes.

Oxygen three-isotope data show that early Earth was mixed after accretion from more heterogeneous material of the Solar Nebula<sup>25</sup>. Analysis of oxygen isotopes in the oldest known rocks places the time of mixing at before 4.0 Ga (ref. 4). The oxygen isotope values ( $\delta^{18}\text{O}=4.8\text{‰}$ ,  $\Delta^{17}\text{O}=0.07\pm 0.12\text{‰}$ ) for the core of zircon 01JH36-69 (Supplementary Appendix 7) are consistent with other Hadean zircons that all fall along the terrestrial fractionation line<sup>26,27</sup>. The new data push the age of any mixing event back 400 Myr to before 4,374 Ma, consistent with formation of a magma ocean by an early moon-forming impact<sup>4</sup> at  $\sim 4.5$  Ga.

Thus, APT data reveal  $\sim 10$ -nm clusters that isolated radiogenic Pb formed between 4.4 and 3.4 Gyr ago, yielding the highest  $^{207}\text{Pb}/^{206}\text{Pb}$  ratios known in zircon. These results explain closed-system behaviour at the 20- $\mu\text{m}$  scale of SIMS analysis while documenting Pb mobility at the nanometre scale, refuting any challenges to the accuracy of SIMS analyses for the age of this zircon based on Pb mobility. The Hadean core of sample 01JH36-69 is the oldest (4,374 Myr old) terrestrial zircon known with multiple age determinations that are all concordant<sup>3,9-13</sup>, confirming the existence of 4.4-Gyr-old zircons from the crust of early Earth. The age of any magma ocean homogenizing Earth's crust and mantle predated the formation of this zircon and thus occurred shortly after formation of the Earth.

## Methods

Analytical technique and references are described in Supplementary Appendix 1 for zircon separation, mounting and polishing, imaging, SIMS analysis and APT.

Sample 01JH36-69 is a detrital zircon ( $\text{ZrSiO}_4$ ) recovered by electric pulse disaggregation of metamorphosed sandstone from the Jack Hills, Western Australia. The zircon was cast in epoxy and polished four times revealing surfaces successively deeper into the  $230 \times 230 \times 430 \mu\text{m}$  prismatic crystal (Fig. 1). Surfaces 1 and 2 were shallow, revealing only the outer portion of the grain. This study reports new data from surfaces 3 and 4, which are closely spaced and exposed the core of the zircon for the first time. These surfaces were imaged by SEM and analysed by SIMS in 10–20- $\mu\text{m}$ -diameter spots, 1 to a few micrometres deep, to determine the age, stable isotope ratios and trace element compositions. Surface 4 was analysed by EBSD. Needle-shaped specimens of zircon were prepared using standard site-specific FIB methods to dimensions of about  $100 \times 100 \times$  up to 1,000 nm for atom-probe analysis; up to  $4 \times 10^8$  ions per specimen were field evaporated into a time-of-flight mass spectrometer and located at subnanometre scale by a position-sensitive detector with an efficiency of  $\sim 37\%$ .

Surface 3 of zircon 01JH36-69 was analysed to determine the U–Pb age using the SHRIMP II ion microprobe at Curtin University with methodology outlined previously. Age determinations involved 7 measurement cycles for each mass, and were calibrated using zircon U–Pb standard CZ3 (age = 564 Myr old; U = 551 ppm). Grains of CZ3 were located within the same epoxy mount as the sample. Five analyses of CZ3 were made, using a 'bracketing strategy', whereby standard analyses were made before, during (between sample analyses 3 and 4) and after analyses of grain 01JH36-69. Data were reduced using the program Squid; sample analyses were corrected for common Pb using measured  $^{204}\text{Pb}$ . The  $2\sigma$  uncertainty in the mean of the Pb/U ratio for the standard analyses was 0.55%. Graphical representations of the U–Pb data were prepared using the program IsoPlot.

Surface 4 of zircon 01JH36-69 was analysed in multiple SIMS sessions to determine the oxygen three-isotope ratios (IMS-1280, UW-Madison,  $\delta^{18}\text{O}$ ,  $\delta^{17}\text{O}$ ); and trace element composition (IMS-1280, UW-Madison). EBSD mapping was performed after SIMS analysis using a Hitachi SU-6600 and Oxford HKL camera (at the University of Western Ontario ZAPLab) at an accelerating voltage of 20 kV and step size of 200 nm. No noise reduction of raw data was performed beyond wildspike correction.

Atom-probe measurements were made using a LEAP 4000X HR at the CAMECA Atom Probe Technology Center, Madison, Wisconsin. Zircon slices measuring  $\sim 3 \times 30 \mu\text{m}$  were removed from the polished face of the crystal and milled to needle-like specimens using a FIB guided by SEM and cathodoluminescence (Fig. 1). Six specimens were obtained from one FIB lift out (Fig. 1a, c). The orientation of each specimen is normal to, and pointing towards, the polished surface in the (100) plane.

The local electrode atom probe (LEAP) is described in detail elsewhere. Using a LEAP, equipped with laser pulsing capability, analysis of bulk insulators has recently become a standard capability. In this instrument, the specimen is a sharp needle cooled to 50 K at high vacuum and a high voltage (typically 4–14 kV) is applied. In this study, a 355-nm-wavelength laser (pulse energy 400 pJ, pulsed at 200 kHz) was focused on the specimen to promote field evaporation of, on average, approximately 0.008 ions per pulse. Ions travel through a time-of-flight mass spectrometer and are recorded by a position-sensitive detector. Each laser pulse starts the clock for time-of-flight. For the specimens used in this study (which measure  $\sim 100$  nm in diameter), the spatial resolution of detected atoms is  $\pm 0.3$  nm in X–Y–Z coordinates. A total of  $6 \times 10^8$  ions were detected;  $2 \times 10^8$  from specimen 1 (R52 126841) and  $4 \times 10^8$  from specimen 2 (R52 126859) at rates of  $\sim 10^7$  ions  $\text{h}^{-1}$ . In principle, all ions are detected with an equal efficiency of  $\sim 37\%$  and a minimum detection limit, determined primarily by the volume of the analysis, of 10 ppma (atomic) for these data. However, spectra must be individually evaluated as some elements ionize poorly or form ionized molecules and isobaric interferences. Mass resolving power is  $\sim 1,000$  (full-width at half-maximum).

Received 15 July 2013; accepted 31 December 2013;  
published online 23 February 2014

## References

- Hanchar, J. M. & Hoskin, P. W. O. Zircon. *Rev. Mineral. Geochem.* **53**, 1–500 (2003).
- Valley, J. W. The origin of habitats. *Geology* **36**, 911–912 (2008).
- Wilde, S. A., Valley, J. W., Peck, W. H. & Graham, C. M. Evidence from detrital zircons for the existence of continental crust and oceans on the Earth 4.4 Gyr ago. *Nature* **409**, 175–178 (2001).
- Rumble, D. et al. The oxygen isotope composition of Earth's oldest rocks and evidence of a terrestrial magma ocean. *Geochem. Geophys. Geosyst.* **14**, 1929–1939 (2013).
- Ewing, R. C. et al. Radiation effects in zircon. *Rev. Mineral. Geochem.* **53**, 387–425 (2003).
- Mattinson, J. M. Zircon U–Pb chemical abrasion ('CA-TIMS') method: combined annealing and multi-step partial dissolution analysis for improved precision and accuracy of zircon ages. *Chem. Geol.* **220**, 47–66 (2005).
- Kusiak, M. A., Whitehouse, M. J., Wilde, S. A., Nemchin, A. A. & Clark, C. Mobilization of radiogenic Pb in zircon revealed by ion imaging: Implications for early Earth geochronology. *Geology* **41**, 291–294 (2013).
- Gault, B., Moody, M. P., Cairney, J. M. & Ringer, S. P. *Atom Probe Microscopy. Springer Series in Materials Science* (Springer, 2012).
- Wyche, S., Nelson, D. R. & Riganti, A. 4350–3130 Ma detrital zircons in the Southern Cross Granite–Greenstone Terrane, Western Australia: Implications for the early evolution of the Yilgarn Craton. *Austral. J. Earth Sci.* **51**, 31–45 (2004).
- Nemchin, A. A., Pidgeon, R. T. & Whitehouse, M. J. Re-evaluation of the origin and evolution of  $>4.2$  Ga zircons from the Jack Hills metasedimentary rocks. *Earth Plan. Sci. Lett.* **244**, 218–233 (2006).
- Holden, P. et al. Mass-spectrometric mining of Hadean zircons by automated SHRIMP multi-collector and single-collector U/Pb zircon age dating: The first 100,000 grains. *Int. J. Mass Spectrom.* **286**, 53–63 (2009).
- Harrison, T. M., Schmitt, A. K., McCulloch, M. T. & Lovera, O. M. Early ( $\geq 4.5$  Ga) formation of terrestrial crust: Lu–Hf,  $\delta^{18}\text{O}$ , and Ti thermometry results for Hadean zircons. *Earth Plan. Sci. Lett.* **268**, 476–486 (2008).
- Cavosie, A. J., Valley, J. W. & Wilde, S. A. in *Earth's Oldest Rocks* (eds van Kranendonk, M. J., Smithies, R. H. & Bennett, V. C.) Devel. Precamb. Geol. **15**, 91–111 (2007).
- Whitehouse, M. J. & Kamber, B. S. On the overabundance of light rare earth elements in terrestrial zircons and its implication for Earth's earliest magmatic differentiation. *Earth Plan. Sci. Lett.* **204**, 333–346 (2002).
- Parrish, R. R. & Noble, S. R. Zircon U–Th–Pb geochronology by isotope dilution—thermal ionization mass spectrometry (ID-TIMS). *Rev. Mineral. Geochem.* **53**, 183–213 (2003).
- Hoskin, P. W. O. Trace-element composition of hydrothermal zircon and the alteration of Hadean zircon from the Jack Hills, Australia. *Geochim. Cosmochim. Acta* **69**, 637–648 (2005).
- Tilton, G. R. Volume diffusion as a mechanism for discordant lead ages. *J. Geophys. Res.* **65**, 178–190 (1960).

18. Nasdala, L. *et al.* Metamictization of natural zircon: Accumulation versus thermal annealing of radioactivity-induced damage. *Contrib. Mineral. Petrol.* **141**, 125–144 (2001).
19. Romer, R. L. Alpha-recoil in U–Pb geochronology: Effective sample size matters. *Contrib. Mineral. Petrol.* **145**, 481–491 (2003).
20. Utsunomiya, S. *et al.* Nanoscale occurrence of Pb in an Archean zircon. *Geochim. Cosmochim. Acta.* **68**, 4679–4686 (2004).
21. Cavosie, A. J., Wilde, S. A., Liu, D., Valley, J. W. & Weiblen, P. W. Internal zoning and U–Th–Pb chemistry of the Jack Hills detrital zircons: a mineral record of early Archean to Mesoproterozoic (4348–1576 Ma) magmatism. *Precamb. Res.* **135**, 231–279 (2004).
22. Valley, J. W. *et al.* Elemental and isotopic tomography at single-atom-scale in 4.0 and 2.4 Ga zircons. *Trans. Am. Geophys. Un.* abstr. V12A-05 (2012).
23. Pidgeon, R. T. & Wilde, S. A. The interpretation of complex zircon U–Pb systems in Archean granitoids and gneisses from the Jack Hills, Narryer Gneiss Terrane, Western Australia. *Precamb. Res.* **91**, 309–332 (1998).
24. Cherniak, D. J. Diffusion in accessory minerals: zircon, titanite, apatite, monazite and xenotime. *Rev. Mineral Geochem.* **72**, 827–869 (2010).
25. Clayton, R. N. Oxygen isotopes in meteorites. *Treat. Geochem.* **1**, 1–14 (2007).
26. Valley, J. W., Ushikubo, T. & Kita, N. T. In situ analysis of three oxygen isotopes and OH in ALH 84001: Further evidence of two generations of carbonates. *Lunar Planet. Sci. Conf.* **38**, abstr. #1147 (2007).
27. Valley, J. W. & Kita, N. T. In situ oxygen isotope geochemistry by ion microprobe. *Min. Assoc. Can.* **41**, 19–63 (2009).

## Acknowledgements

This research was supported by NSF-EAR0838058, DOE-93ER14389 and the NASA Astrobiology Institute. T.C., D.R., D.F.L., D.J.L. and P.C. thank their colleagues at CAMECA in Madison, Wisconsin, for their contribution to these efforts. WiscSIMS is partly supported by NSF-EAR1053466.

## Author contributions

J.V. initiated this project, selected samples, assisted in data reduction and interpretation, and wrote most of the paper. A.C. and S.W. dated the 4.4-Gyr-old zircon by SIMS, and assisted in interpretation and rewriting. TU made SIMS analysis of trace elements and SEM images, and assisted in interpretation. D.R. performed data analysis of APT data, and assisted in interpretation. D.F.L. prepared samples by FIB. D.J.L., P.C. and T.K. performed atom-probe analysis and assisted in interpretation. D.M. conducted EBSD analysis and SEM imaging of the zircon. M.S. assisted in analysis and interpretation. All authors reviewed and approved this paper.

## Additional information

Supplementary information is available in the [online version of the paper](#). Reprints and permissions information is available online at [www.nature.com/reprints](http://www.nature.com/reprints). Correspondence and requests for materials should be addressed to J.W.V.

## Competing financial interests

The authors declare competing financial interests: details accompany the paper at <http://www.nature.com/naturegeoscience>